Assessment of a planar inclusion in a solid cylinder

M. Imran [a], S.F. Eric Lim [a], I.S. Putra [b], A.K. Ariffin [c], C.J. Tan [a], J. Purbolaksono [a,*]

[a] Centre of Advanced Manufacturing and Materials Processing, Department of Engineering Design & Manufacture, Faculty of Engineering, University of Malaya, Kuala Lumpur 50603, Malaysia
[b] Department of Aeronautics and Astronautics, Institute of Technology Bandung, Bandung 40132, Indonesia
[c] Department of Mechanical and Materials Engineering, Faculty of Engineering and Built Environment, Universiti Kebangsaan Malaysia, Bangi 43600, Selangor, Malaysia

ARTICLE INFO

Article history:
Received 18 August 2014
Received in revised form 22 November 2014
Accepted 26 November 2014
Available online 11 December 2014

Keywords:
Stress intensity factor
Planar inclusion
Embedded crack
Dual boundary element method

ABSTRACT

As a planar inclusion in a solid cylinder can lead to a catastrophic failure of a whole structure, relevant studies on evaluating quantitative fracture values are always sought for supporting the investigations. In line with the use of nondestructive evaluation technique for quantifying the embedded defects in structures, relevant research findings would be usable to contribute to the structural integrity analyses. It is also intended to have the possibility of the use of the data in a preliminary structural design stage. Since the complexity of the experimental setup for evaluating a planar inclusion in a solid component, numerical modeling is always desirable. There are currently very few available solutions of stress intensity factors for the embedded cracks in a solid cylinder in literature. In this work, the planar inclusion was considered as an embedded (penny/elliptical) crack. Stress intensity factors (SIFs) of an embedded crack for different crack aspect ratios, crack eccentricities and crack inclinations are presented. All the analyses were carried out by using a dual boundary element method (DBEM) based software.

1. Introduction

Solid cylinder has been widely used in the engineering components and structures. They are usually used as rods, stands, shafts and chords. In practices, there are always some inherent micro cracks in structures due to metallurgical defects or production processes. These defects cause the reduction of mechanical strength of the cylinder and can lead to a catastrophic failure of the structure. Since fracture mechanics perspective has widely been adopted in engineering design process, studies on the stress intensity factor have become necessary, especially the possibility of the use of the data in a preliminary design stage. Also, to support the use of nondestructive technique for evaluating the embedded defects in structures, the relevant solutions/data are always sought.

A number of studies on surface cracks have been widely reported by many researchers. Citarella and Cricri [1] evaluated SIFs for two bird-wing cracks emanating from circumferential notch of a solid cylinder subjected to remote torsion by using dual boundary element (DBEM) and finite element method (FEM). The DBEM and FEM results were reported to be in good agreements. Noda and Takase [2] proposed analytical SIFs solutions for a V-shape round specimen under torsion, tension and

* Corresponding author. Tel.: +60 3 79675341.
E-mail address: judha@um.edu.my (J. Purbolaksono).

http://dx.doi.org/10.1016/j.engfailanal.2014.11.027
1350-6307/

bending loadings. They reported that the normalized SIFs were shown to be largely dependent on notch depth. Chen [3,4] studied multiple cracks in a rectangular bar and a thin-walled cylinder subjected to torsion loading using the finite difference method.

In past few years, significant efforts have been devoted to provide solutions for stress distribution, notch stress concentration factor and stress intensity factor [5,6]. Recently, Ismail et al. [7] presented a number of the SIF results for surface cracks in round bar under bending, torsion and mixed-mode loadings. Predan et al. [8] reported the SIFs for Modes II and III of semi-elliptical surface cracks in a hollow cylinder under torsion using a finite-element technique. Malits [9] proposed an efficient solution for evaluating the SIFs of a circumferential edge crack in a solid cylinder.

However, there are only few works on embedded elliptical crack in solid cylinders that have been reported in literature [10]. This statement is supported by Atroshchenko et al. [11], saying that embedded elliptical crack are more complicated and challenging in crack geometry compared to surface cracks. A famous early solution for embedded crack was reported by Newman and Raju [12]. They used the finite element method to evaluate the SIFs of an embedded elliptical crack in a prismatic bar. Wang and Glinka [13] evaluated stress intensity factors of embedded elliptical cracks under complex two-dimensional loading conditions using weight function method. Based on the properties of weight functions and the available weight functions for two-dimensional cracks, new mathematical expressions using the point load weight function were proposed. Montenegro et al. [14] used the O-integral algorithm and the weight function methodology for evaluating SIFs of embedded plane cracks. Qian [15] studied effects of crack aspect ratio, crack eccentricity and effect of pipe thickness of embedded elliptical crack axially oriented in a pressurized pipe using the interaction integral approach for three-dimensional finite element crack front model.

In this work, the normalized SIFs of a planar inclusion, that is modeled as an embedded crack, for different crack aspect ratios, crack inclinations and eccentricities in a solid cylinder under tension and torsion loading are presented. Relevant benchmarking model is also presented for comparison. Here, all the analyses are carried out by using the boundary element software package of BEASY [16].

2. Materials and method

A 20 mm-diameter solid cylinder with100 mm in length is used in this study. A tensile stress of 100 MPa for tension loading and a maximum shear stress of 100 MPa ($M_t = 530 \times 10^3$ N mm) for torsion loading are used in all cases for calculating the SIFs except those for the benchmarking models. The J-integral method is used to evaluate the stress intensity factors. The material used in this study is mild steel with modulus of elasticity $E = 210$ GPa and Poisson's ratio $\nu = 0.29$. The parameters and notations used for the embedded crack and the J-integral paths are depicted in Fig. 1. An embedded crack for different aspect ratios b/a is introduced in the mid-axis of the solid cylinder, and the corresponding SIFs are evaluated. Next, the effects of the crack inclination and the crack eccentricity shifting from the axis on the SIFs under both tension and torsion loadings are studied.

BEASY [16] software uses the DBEM which was developed by Mi and Aliabadi [17] for treating the crack boundaries. The displacement and traction boundary integral equations are written, respectively, as [17]

$$C_{ij}(x')u_j(x') = \int_S U_{ij}(x',x)t_j(x)dS - \int_S T_{ij}(x',x)u_j(x)dS \tag{1}$$

$$\frac{1}{2}t_j(x') + n_i(x')\int_S S_{kij}(x',x)u_k(x)dS = n_i(x')\int_S D_{kij}(x',x)t_k(x)dS \tag{2}$$

where x' and x are the source point and boundary point, respectively, the notations i and j are the Cartesian components, n is the outward normal vector, S denotes the domain surface, U_{ij} and T_{ij} are the Kelvin fundamental solutions, S_{kij} and D_{kij} contain the derivatives of U_{ij} and T_{ij}, respectively, the coefficient C_{ij} is given by δ_{ii} (Kronecker delta function) for a smooth boundary at x'. Next, the modeling strategy of three-dimensional crack problems may be summarized as follows [17]:

- Crack surfaces are modeled with discontinuous elements.
- Surfaces intersecting a crack surface are modeled with edge-discontinuous quadrilateral or triangular elements.
- The traction integral equation (Eq. (2)) is applied for collocation on the opposite crack surface, i.e. the lower surface.
- The displacement integral equation (Eq. (1)) is applied for collocation on one of the crack surfaces, i.e. the upper surface, and for the other surfaces.

In order to have fine meshing for convergence, consideration has to be taken on the ratio of the neighboring elements shall not be more than five times its size. The element size on the crack front of the embedded crack is set to be smaller than one fifth of the embedded crack size.

3. Numerical results and discussion

To demonstrate the accuracy of the results obtained by using BEASY [16], the SIFs of an embedded crack for different aspect ratios ($b/a = 0.4$, 1, and 2) in a rectangular bar are validated with the Newman and Raju' solution [12] that was derived

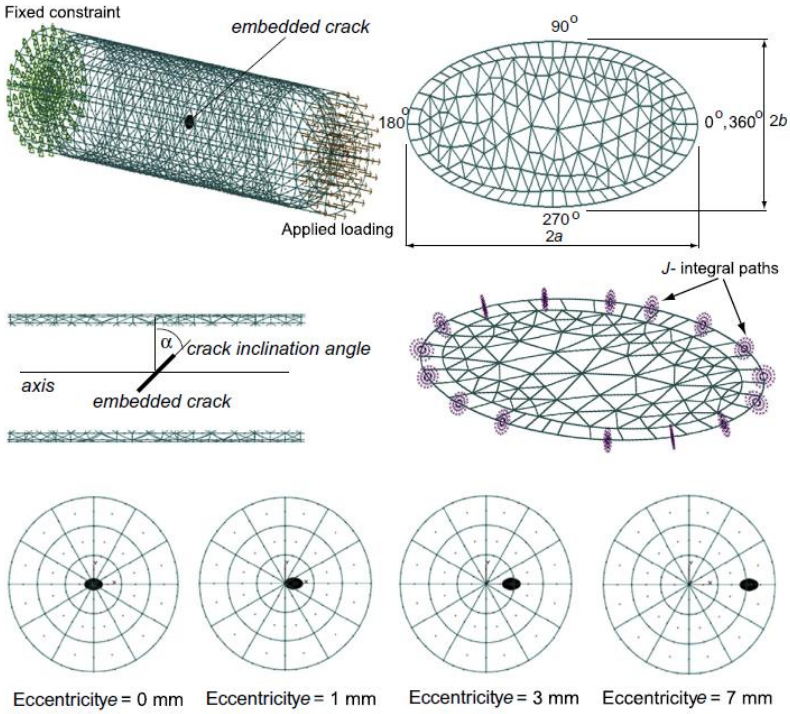

Fig. 1. The model of an embedded crack in a solid cylinder and the parameters and notations used in the simulations.

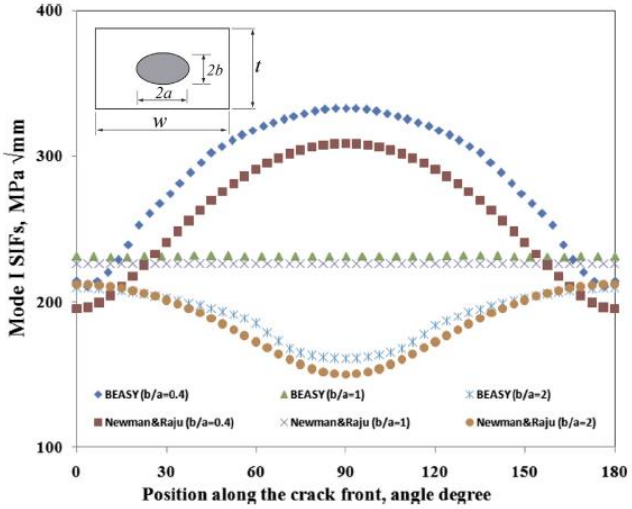

Fig. 2. The Mode I SIFs of an embedded crack for different aspect ratios (b/a = 0.4, 1, and 2) in a rectangular bar by BEASY [16] and Newman and Raju [12].

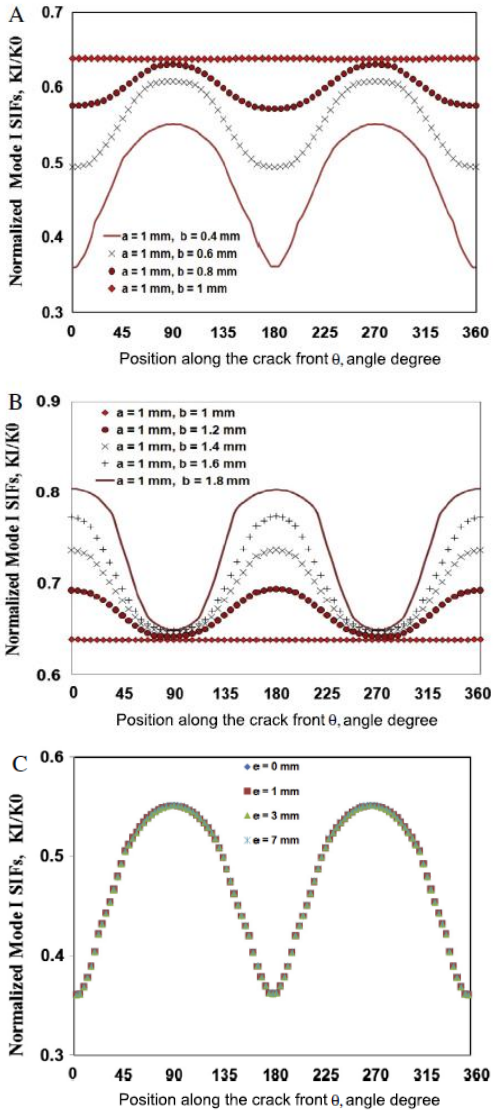

Fig. 3. (A) Normalized Mode I SIFs K_I/K_0 for $b/a \leqslant 1$; (B) normalized Mode I SIFs K_I/K_0 for $b/a \geqslant 1$; (C) normalized Mode I SIFs K_I/K_0 for different crack eccentricities.

based on the finite element results. The crack depth b is set to be 1 mm. The bar has 30 mm in width and 10 mm in thickness and is subjected to a tensile stress of 200 MPa. The Mode I SIFs along the crack front are presented in Fig. 2. Both results are shown to be in good agreements. Next, the effects of crack aspect ratios, crack eccentricities and inclinations on the SIFs under tension and torsion loading are presented in the following sections. The SIFs are normalized with a parameter of $K_o(=\mathrm{T}\sqrt{\pi(a)})$, where T is the applied tension/torsion stress (=100 MPa) and a is the crack length (=1 mm).

3.1. Crack aspect ratio under tension loading

It can be observed from Fig. 3A and B that larger Mode I SIFs along the crack front are found at the smaller crack length a or crack depth b. For a given b/a, the smaller size in length or depth of a part-through/embedded crack exaggerates a

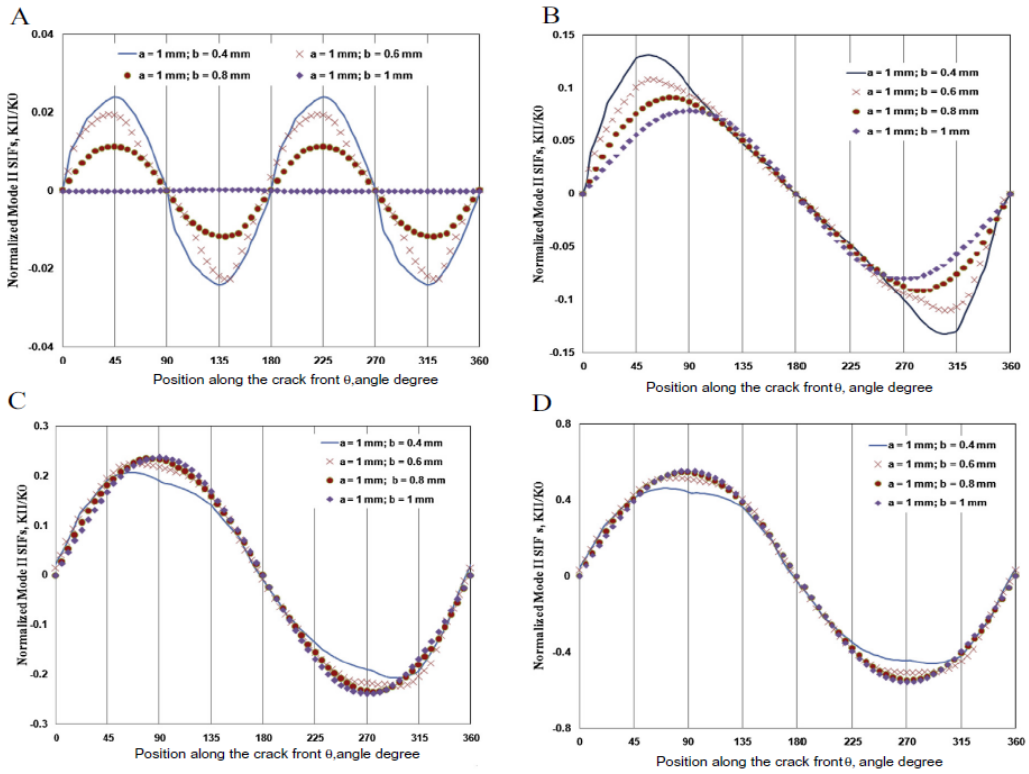

Fig. 4. Effect of crack eccentricity e on Mode II SIFs for different crack aspect ratio ($b/a \leqslant 1$): (A) $e = 0$ mm; (B) $e = 1$ mm; (C) $e = 3$ mm; (D) $e = 7$ mm.

geometrical effect on the crack front to produce a larger principal stress at its surrounding. Modes II and III SIFs are known to be negligible for the crack inclination $\alpha = 0$. Fig. 3C shows the SIFs of embedded crack ($b/a = 0.4$) for different crack eccentricities e. It is shown that there is no effect of the crack eccentricity on the SIFs. It is likely due to the nature of uniform tensile stress distribution at the cross section. Thus, the effect of crack eccentricity on the SIFs is expected to be different if the loading is either bending or torsion.

3.2. Crack aspect ratio under torsion loading

The normalized Mode II SIFs for different crack aspect ratios and eccentricities with $\alpha = 0$ are presented in Figs. 4 and 5. It is known that torsion loading would produce linearly distributed shear stress from the axis to the surface as a function of the cylinder radius. Under torsion loading, Mode I SIFs are known to be negligible for the crack inclination $\alpha = 0$. The normalized Mode II SIFs along the crack front for $b/a = 1$ (a penny crack) and $e = 0$ mm under torsion loading are shown to be close to zero (Figs. 4A and 5A). This is due to the shear stress acting uniformly and tangentially along the crack front of a penny crack, leading to no slip activities. For crack eccentricity $e = 0$ mm, the normalized Mode II SIFs along the crack front of the elliptical cracks are shown to form a two-cycle wave (Figs. 4A and 5A). At $e = 0$ mm, both crack geometry and shear stress distribution are symmetric. Thus, the torsion shear stress would produce symmetrical states of stress about the major and minor axes of the crack front, resulting in two-cycle-wave pattern. As the crack center is shifting from the cylinder axis ($e \neq 0$), the shear stress distribution due to torsion is only symmetric about either major or minor axis which is parallel to the radial direction. Thus, the patterns of the SIFs along the crack front change to form a single-cycle wave as shown in Figs. 4B–D and 5B–D.

In general, at $e = 0$ mm, a crack aspect ratio b/a which is further from unity would result in larger SIFs (Figs. 4A and 5A). At $e = 1$ mm, the inner half of the crack front is subjected to small shear stresses, resulting in insignificant difference on the SIFs (Fig. 4B). Meanwhile, its outer half has more distortion, causing the significant effect of the crack aspect ratio

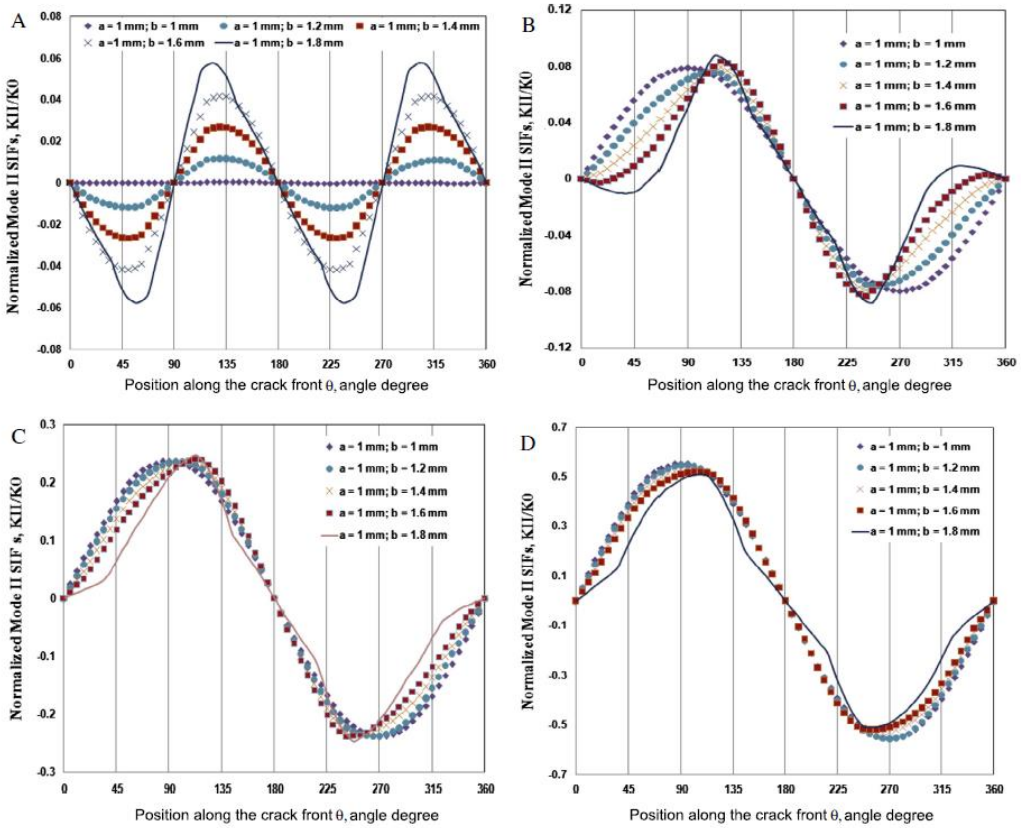

Fig. 5. Effect of crack eccentricity e on Mode II SIFs for different crack aspect ratio ($b/a \geqslant 1$): (A) $e = 0$ mm; (B) $e = 1$ mm; (C) $e = 3$ mm; (D) $e = 7$ mm.

on the SIFs. For $b/a < 1$ and larger eccentricities ($e = 3$ mm and 7 mm), effect of the crack aspect ratio on the SIFs distribution on the crack front becomes less significant (Fig. 4C and D). It may be noted that since the size of the crack is relatively small in comparison to the cylinder radius, the shear stress distribution between the inner and outer points of the crack front would have less difference. Meanwhile, in comparison to the Mode II SIFs presented in Fig. 4C and D, the SIFs for $b/a > 1$ (Fig. 5C and D) have skewed with different degree depending on the crack aspect ratio b/a. It may be noted that for $b/a < 1$, the shear stress distribution only discontinues across the major axis of the crack (in radial direction). Meanwhile, for $b/a > 1$, the shear stress distribution discontinues in mixed direction due to the orientation of the major and minor axes of the embedded crack.

Figs. 6 and 7 show the effect of the crack eccentricities on the Mode III SIFs for different crack aspect ratios of $b/a \leqslant 1$ and $b/a \geqslant 1$. At $e = 0$ mm, the normalized Mode III SIFs show waving patterns with the absolute maximum values at $\theta = 0°$ (360°) and 180° for $b/a \leqslant 1$ and at $\theta = 90°$ and 270° for $b/a \geqslant 1$. These features are due to the geometrical effect at the shorter axis of the crack front to produce larger principal stresses. Similarly, a larger b/a is shown to result in larger SIFs. The SIFs for the penny crack ($b/a = 1$) are found to be about constant due to uniform tearing stress along the crack front.

When the crack center is shifting from the axis, the pattern of the Mode III SIFs has evolved to identically form a parabolic curve (Figs. 6B–D and 7B–D). It may be explained that since the shear stress increases towards the outer surface and the tearing force is greatly influenced by the principal stress at the free-crack cross section around the crack front, the absolute maximum Mode III SIFs for $e \neq 0$ are generally found at $\theta = 0°$ (360°). It can be observed from Figs. 6B–D and 7B–D, the ratios of the SIF values at the inner (180°) and outer (0/360°) points would tend to be unity as the crack center approaches the cylinder surface. If the crack center is further approaching the outer surface, the principal stresses at the free-crack cross section around the crack front (0° and 180°) have less difference. However, this is also depending on the size of crack. Also, as the crack eccentricity increases, the mid-section of the crack front (90° and 270°) would have states of stress that give less